water

Article

Study on Influencing Parameters of Total Phosphorus Degradation in Cattle Farm Wastewater by Electrocoagulation Using Magnesium, Aluminum, and Iron Electrodes

Peng Chen, Junfeng Li * and Ningning Xie

College of Water Conservancy and Architectural Engineering, Shihezi University, Shihezi 832000, China; chenpeng9798@163.com (P.C.); xnn2690@163.com (N.X.)
* Correspondence: ljfshz@126.com

Abstract: Magnesium, aluminum, and iron electrode were common anodes in electrocoagulation (EC), but there were few studies comparing the influence of operating parameters on the reaction and the effects of these three different anodes in removing total phosphorus (TP) in cattle farm wastewater (CFW). This study used these three different electrodes as the anode of the electrocoagulation method. The operating parameters such as electrode distance (ED), initial pH, and voltage were examined by the Taguchi method and single-factor method. The result of Taguchi analysis shows that voltage has a significant impact on TP removal of magnesium (Mg) and aluminum anode (Al), and ED has a significant impact on TP removal of magnesium and iron anode (Fe). Among the three operating parameters, the first in the order of the impact on the reaction was ED because ED has the greatest influence on the dissolution of the anode. The result of single-factor analysis shows that the optimum conditions of Mg were ED = 3 cm, voltage = 5 V, pH = 7, Al were ED = 3 cm, voltage = 5 V, pH = 5, and Fe were ED = 3 cm, voltage = 5 V, and pH = 7. For Mg and Fe, the voltage and reaction results follow the second-order reaction kinetics, and Al is the first-order reaction kinetics. Through comparison of the three anodes, it was found that Al worked best in actual CFW. It was noted that the conditions obtained by the single-factor method were more economical in the treatment of actual CFW. This work could provide reference for determining the extent of the influence of operating parameters when other contaminants are removed, and provide reference for comparing the other anodes in EC.

Keywords: total phosphorus; three different anodes; operating parameters; Taguchi method; single-factor method

check for updates

Citation: Chen, P.; Li, J.; Xie, N. Study on Influencing Parameters of Total Phosphorus Degradation in Cattle Farm Wastewater by Electrocoagulation Using Magnesium, Aluminum, and Iron Electrodes. *Water* **2023**, *15*, 4134. https://doi.org/10.3390/w15234134

Academic Editors: Giovanni Esposito and Danny D. Reible

Received: 15 October 2023
Revised: 15 November 2023
Accepted: 27 November 2023
Published: 29 November 2023

Copyright: © 2023 by the authors. Licensee MDPI, Basel, Switzerland. This article is an open access article distributed under the terms and conditions of the Creative Commons Attribution (CC BY) license (https://creativecommons.org/licenses/by/4.0/).

1. Introduction

In recent years, the discharge of domestic sewage and industrial wastewater increased with the development of the economy and the increase in population, which resulted in more and more serious nitrogen and phosphorus pollution in the water environment. The excessive discharge of phosphorus wastewater causes the eutrophication of the water environment, which leads to the frequent occurrence of eutrophication [1]. This caused grave damage to the natural water ecological environment and threatened human health [2]. In particular, the wastewater from the aquaculture industry contains a lot of phosphorus-containing pollutants, and it is easy to discharge into the natural water environment. Farming wastewater (FW) generally contains a large amount of animal manure, urine, small particle feed, antibiotics [3], etc. The feces and urine contain a lot of nitrogen and phosphorus. According to China's second pollution source survey, the phosphorus content in wastewater from the aquaculture industry amounted to 212,000 tons [4]. Therefore, the removal of phosphorus from wastewater became a research hotspot in the field of water treatment.

The common methods of phosphorus removal in wastewater include the physical method, chemical method, and biological method. The sensible method was mainly to remove phosphorus through adsorbents, or to remove phosphorus-rich sludge in water, which is simple and easy to operate [5–7]. Industrial solid wastes such as coal slag and steel slag were applied to adsorb phosphorus in water with good results [8,9]. In addition, a large number of new adsorbents with nanostructures were also used to remove phosphorus from water, such as iron-zirconium-modified activated carbon nanotube, $La(OH)_3/Fe_3O_4$ nanocomposites and La-porous carbon composites [10–12]. However, there were further disadvantages, such as the high cost of adsorbent, poor circulation, and the possibility of destroying the nitrogen and phosphorus balance of the water body. The principle of the chemical method is that the inorganic metal salt agent added to the wastewater reacts with phosphorus pollutants such as phosphate to produce insoluble phosphate precipitates; and finally, the phosphorus in the wastewater is removed through solid–liquid separation. Huang et al. investigated three metal salts ($AlCl_3$, $CaCl_2$, and $MgCl_2$) to recover phosphate form anaerobic digestion supernatant of sludge [13]. Kubar et al. studied some common salts ($ZnCl_2$, $FeCl_3$, $FeCl_2$, $CuCl_2$, Na_2CO_3, and $NaHCO_3$) from biogas slurry [14]. It can be seen that chemical phosphorus removal can achieve excellent results. However, the large amount of chemical agents added in the treatment process can produce a large amount of flocculent sludge, which may cause secondary pollution, and the chemical method also has the disadvantages of a larger area and high cost. Biological phosphorus removal methods are through the metabolism of denitrifying phosphorus-accumulating and phosphate-accumulating bacteria [15,16]. However, in practical applications, the biological method exposes two major disadvantages: (1) the treatment time is longer and the phosphorus removal effect is insignificant; (2) the treatment cost of the remaining phosphorus-containing sludge is higher [17,18]. Therefore, it is necessary to develop a phosphorus removal technology with straightforward operation, low cost, small footprint, and high treatment efficiency.

Electrochemical (EC) water treatment technology has the advantages of environmental friendliness, low cost, simple structure, convenient operation [19], etc., which attracted wide attention of researchers. EC uses electric current to address and flocculate pollutants without adding flocculants. EC was a technique wherein the anode energization leads to the release of metal cations into wastewater, facilitating the formation of flocculates consisting of metal cations and hydroxide ions that effectively adsorb pollutants present in the wastewater. In comparison to electro-oxidation, electroflocculation exhibits superior capability in removing inorganic substances from wastewater. EC mainly removes pollutants in water through the following ways: (i) anodic dissolution, (ii) hydroxyl polymer formation, and (iii) pollutant precipitation [19–21].

At present, electrocoagulation technology was applied to treat a variety of difficult-to-treat wastewater. Electrocoagulation has a good treatment effect on a variety of pollutants, such as poultry wastewater [22], cattle slaughter wastewater [23], tannery wastewater [24], laundry wastewater [25], restaurant wastewater [26], silica [27], and microalgae [28] dyes and textile wastewater [29–33], heavy metal [34–37], oil, and grease [38–41]. In addition, electrocoagulation technology was also applied to remove phosphorus pollutants from wastewater. Gao et al. utilized double iron electrodes to build an electrocoagulation reactor, and the phosphorus removal rate reached 100% under the best conditions [42]. Liu et al. used magnesium as the anode of the electrocoagulation reactor, which can remove 80% of the TP in 60 min [43]. Mores et al. used a continuous flow electrocoagulation reactor to treat pig farm wastewater, the phosphorus removal rate of the iron anode electrocoagulation reactor was 96%, and that of the aluminum anode electrocoagulation reactor was 93% [44]. It can be observed that electrocoagulation technology can efficiently remove phosphorus pollutants in FW.

The anodes used in electrocoagulation reactors were mainly metals such as magnesium anode (Mg), aluminum anode (Al), and iron anode (Fe). However, at present, assessing the performance of different metal anode electrocoagulation reactors for the treatment of phosphorus pollutants in FW was few.

According to Kobya et al. [45] the operating parameters such as ED, initial pH, and voltage were the main parameters. However, there was little research on the relationship between parameter levels and reaction results.

In the study, Mg, Al, and Fe were employed in EC reactor, respectively, in order to investigative the following issues:

(1) The relationship between three reaction parameters (ED, pH, and voltage) and the removal of TP in simulated cattle farm wastewater (SCFW).

(2) The optimal reaction conditions for withdrawing the parameters of TP in SCFW.

(3) Determining which of the three metal anodes are more suitable for actual cattle farm wastewater (ACFW).

2. Materials and Methods

2.1. Chemicals and Materials

Sodium hydroxide (NaOH, ≥96.0%, Zhiyuan Chemical Reagent Co., Ltd., Tianjin, China) and hydrochloric acid (HCl, 37%, Zhiyuan Chemical Reagent Co., Ltd., Tianjin, China) were used to adjust the pH. Sodium chloride (NaCl, ≥99.5%, Zhiyuan Chemical Reagent Co., Ltd., Tianjin, China) was used as an electrolyte. Potassium dihydrogen phosphate (KH_2PO_4, ≥99.5%, Zhiyuan Chemical Reagent Co., Ltd., Tianjin, China) was used to prepare phosphorus wastewater. Ascorbic acid ($C_6H_8O_6$, >99.0%, Zhiyuan Chemical Reagent Co., Ltd., Tianjin, China), ammonium molybdate ($(NH_4)_6Mo_7O_{24}\cdot 4H_2O$, ≥99.0%, Zhiyuan Chemical Reagent Co., Ltd., Tianjin, China), and potassium antimony tartrate ($K(SbO)C_4H_4O_6\cdot 1/2H_2O$, ≥99.0%, Zhiyuan Chemical Reagent Co., Ltd., Tianjin, China) were used to measure the TP content of the solution. Potassium dichromate ($K_2Cr_2O_7$, ≥99.8%, Zhiyuan Chemical Reagent Co., Ltd., Tianjin, China), sulfuric acid (H_2SO_4, 98%, Zhiyuan Chemical Reagent Co., Ltd., Tianjin, China), phenanthroline ($C_{12}H_8N_2\cdot H_2O$, ≥99.0%, Zhiyuan Chemical Reagent Co., Ltd., Tianjin, China), ferrous sulfate ($FeSO_4\cdot 7H_2O$, ≥99.0%, Zhiyuan Chemical Reagent Co., Ltd., Tianjin, China), ferrous ammonium sulfate ($(NH_4)_2Fe(SO_4)_2\cdot 6H_2O$, ≥99.5%, Zhiyuan Chemical Reagent Co., Ltd., Tianjin, China), and silver sulfate (Ag_2SO_4, ≥99.7%, Zhiyuan Chemical Reagent Co., Ltd., Tianjin, China) were used to measure the COD of the solution.

2.2. Experimental Setup

The experiments were conducted in a glass reactor containing 500 mL of experimental CFW as shown in Figure 1.

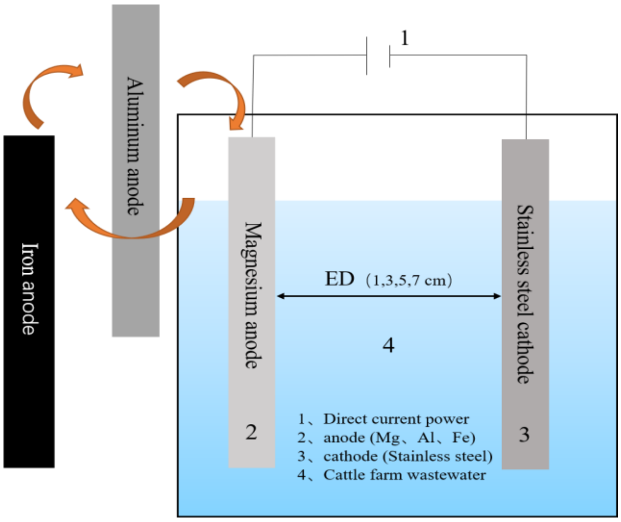

Figure 1. Schematic diagram of electrocoagulation reactor.

Experimental CFW included SCFW and ACFW. SCFW consisted of 150 mg·L^{-1} TP. ACFW was collected from cow dung rinse water of a farm located in Shihezi, China. The physicochemical indexes of ACFW were shown in Table 1.

Table 1. Physicochemical indexes of actual aquaculture.

Test Items	Value	Unit
Total phosphorus	16.43~17.01	mg·L^{-1}
pH	8	-
COD	560.64~579.33	mg·L^{-1}
BOD_5	108	mg·L^{-1}
Conductivity	922	µS·cm^{-1}

The operational parameters such as voltage, ED, and pH were investigated using the Taguchi method by MINITAB statistical package 17.0 version [46], which includes range analysis, data normality analysis, Box–Cox change analysis, one-way analysis of variance (ANOVA), Kruskal–Wallis method analysis, and main effect analysis. The Taguchi method was applied to analyze the SCAW through changing the operational parameters with the different level [voltage (3, 5, 7, and 9 V), ED (1, 3, 5, and 7 cm), and pH (5, 7, 9, and 11)].

As shown in Figure 1, the anodes were Al, Fe, and Mg, respectively. NaCl (2.922 g) was inserted into wastewater as an electrolyte. The sizes of the three electrodes were 7 cm × 6 cm × 0.4 cm. Energy was provided by a direct current power (MS-605D, Hongyou Instrument Co., Ltd., Shanghai, China). During the experimental, samples were harvested by centrifuge tube every 10 min. Aiming to increase the accuracy, each experiment was repeated three times.

2.3. Analytical Methods

The concentration of TP was measured by a UV spectrophotometer (DR6000, HACH, Loveland, CO, USA) at 700 nm [47] after centrifugal by centrifuge (TGL-18000Cr, Anting Science Co., Ltd., Shanghai, China), and removal efficiency was calculated using Equation (1):

$$\text{TP removal}(\%) = (C_0 - C_t)/C_0 \times 100\% \tag{1}$$

where C_0 and C_t were the initial concentration (mg·L^{-1}) and the concentration at time t (mg·L^{-1}) of the CAW, respectively.

Anode consumption was calculated using Equation (2):

$$\text{Anode consumption(mg)} = m_0 - m_t \tag{2}$$

where m_0 and m_t were initial quality (mg) and the quality at time t (mg).

Chemistry oxygen demand (COD) was measured by the potassium dichromate digestion method, and COD_{Cr} content was calculated using Equation (3):

$$W_{COD}(mg \cdot L^{-1}) = [(V_0 - V_1) \times C \times 8 \times 1000]/10 \tag{3}$$

where V_0 and V_1 were the amount of $(NH_4)_2Fe(SO_4)_2 \bullet 6H_2O$ consumed by the control group and experiment group (ml), C is the concentration of $(NH_4)_2Fe(SO_4)_2 \bullet 6H_2O$, and this research C = 0.0584 mol·L^{-1}. The electric energy consumed can be calculated using Equation (4):

$$EC(kW \cdot h) = U \times I \times t \tag{4}$$

where t is the treat time (h), U is the voltage of treat (V), and I is the current of treat (A).

The kinetics study was conducted using first-order and second-order models [48]. The first-order model is analyzed as follows with Equation (5):

$$In[q_e - q_t] = Inq_e - K_1 \times t \tag{5}$$

where q_e and qt are the amounts of TP adsorbed at equilibrium sorption capacity and time t, respectively. K_1 (min^{-1}) is the reaction rate constants of first order.

The second-order model can be calculated using Equation (6):

$$t/q_t = 1/(K_2 \times q_{e2}) - t/q_t \tag{6}$$

where k_2 (min^{-1}) is the reaction rate constants of second-order.

Field emission scanning electron microscopy (SEM, Fei Quanta 650FEG, Yuan Haiwei Passenger Aircraft Co., Ltd., Beijing, China) with energy-dispersive X-ray spectroscopy (EDX) was used to obtain the morphologies and elemental compositions of the sludge sample and electrodes. The pH of wastewater was measured with a water quality analyzer (SL-1000, HACH, USA).

3. Results and Discussion

3.1. Taguchi Method Analysis

The removal efficiency and anode consumption were obtained for Mg, Al, and Fe as shown in Table 2.

Table 2. The removal efficiency of TP and anode consumption using Mg, Al, and Fe.

Run	Independent Variable			TP Removal (%)			Anode Consumption (mg)		
	ED	pH	Voltage	Mg	Al	Fe	Mg	Al	Fe
1	1	5	3	87.60	80.06	40.23	3.79	2.31	5.08
2	1	7	5	95.17	75.50	40.08	8.01	4.39	8.01
3	1	9	7	74.85	82.91	37.18	8.21	7.12	10.11
4	1	11	9	86.26	81.07	22.58	13.64	7.48	12.96
5	3	5	5	85.54	94.56	17.58	3.50	1.52	4.48
6	3	7	3	95.14	64.60	33.80	1.61	0.78	2.12
7	3	9	9	82.92	83.33	21.38	5.11	3.75	3.80
8	3	11	7	63.84	82.33	19.02	2.90	2.64	5.78
9	5	5	7	95.32	76.35	22.62	4.21	1.92	5.53
10	5	7	9	78.86	91.08	31.33	5.16	2.40	6.00
11	5	9	3	79.61	10.66	12.30	1.50	0.60	1.62
12	5	11	5	80.82	83.42	18.36	2.36	1.21	3.05
13	7	5	9	77.75	67.52	18.07	3.32	1.79	4.32
14	7	7	7	72.80	26.23	17.61	2.73	1.33	3.13
15	7	9	5	75.77	40.09	15.35	1.87	0.87	2.02
16	7	11	3	79.49	61.67	36.28	0.73	0.42	1.01

The result of the average range analysis of TP removal is presented in Tables S1–S3. As for Mg, the average range of ED was 14.93, pH was 4.52, and voltage was 14.55. In case of Al, the average range of ED was 40.65, pH was 18.04, and voltage was 38.09. As for Fe, the average ranges of three operating parameters were 17.07, 6.15, and 15.34, respectively. Therefore, for three anodes, the degree of influence of the reaction conditions was ED > voltage > pH. This could be because these three parameters have other effects on anode dissolution.

The result of the average range analysis of anode consumption is shown in Tables S4–S6. It was clearly that the influence of ED on anode consumption was greater than the influence of pH and voltage. Therefore, it can be determined that the effect of ED on the removal of TP in wastewater was ranked first because it has the greatest impact on anode dissolution, followed by voltage and pH.

In addition, through normal analysis (Figure 2), it was clearly shown that the *p*-value of Mg was >0.100, Al was <0.010, and Fe was 0.071. Therefore, Mg and Fe comply with the customary distribution, but Al was incompatible, and in the Box–Cox (Figure 3), the confidence interval was 95%. It could be summarized that the optimal λ-value was 1.04, and 1.04 was within the 95% confidence interval (0.17~2.43). This implies that the result of Al was not suitable for the Box–Cox change. Therefore, the relationship between the TP removal effect of Mg and Fe could be tested by ANOVA, while Al could be analyzed by Kruskal–Wallis method analysis [49].

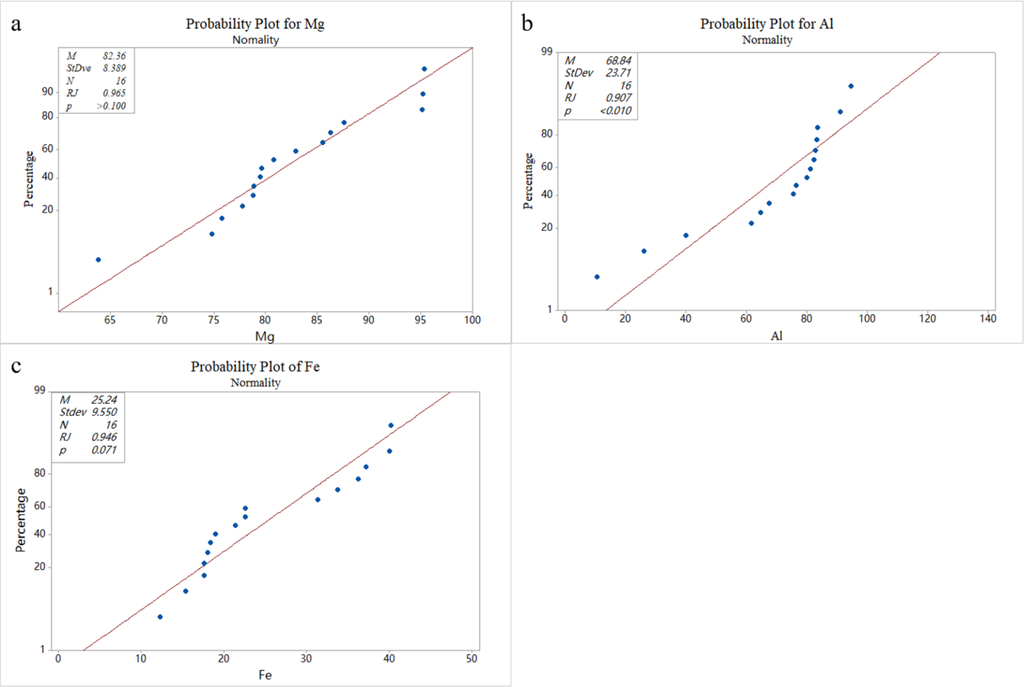

Figure 2. The normal analysis diagram of the TP removal effect of the three anodes in the Taguchi analysis table ((**a**) Mg, (**b**) Al, and (**c**) Fe).

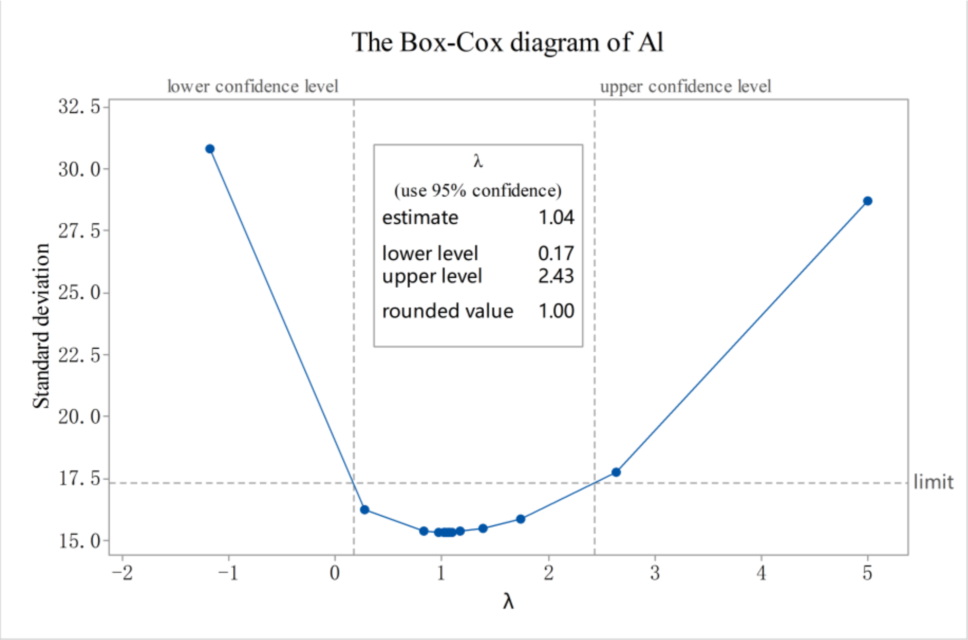

Figure 3. The result of Box–Cox of Al.

The results are shown in Table 3, the *p*-value < 0.05 of Mg was ED and voltage, Al was voltage, and Fe was ED. It could be concluded that voltage has a significant effect on the removal of Mg and Al, and ED has a significant effect on the removal of Mg and Fe.

Table 3. The relationship between the operating parameters and removal efficiency of TP.

Source	***p*-Value**		
	Mg	**Al**	**Fe**
ED	0.045	0.229	0.048
pH	0.901	0.993	0.838
voltage	0.048	0.016	0.076

Through Taguchi method analysis, the optimum parameter level of the three anodes could conclude. As shown in the Figure 4, the highest point in the linear graphs obtained was selected as the optimum parameter level. It was clear that the optimum parameter level of Mg was ED = 1 cm, pH = 9, voltage = 9 V, Al was ED = 1 cm, pH = 7, voltage = 9 V, and Fe was ED = 1 cm, pH = 9, and voltage = 9 V.

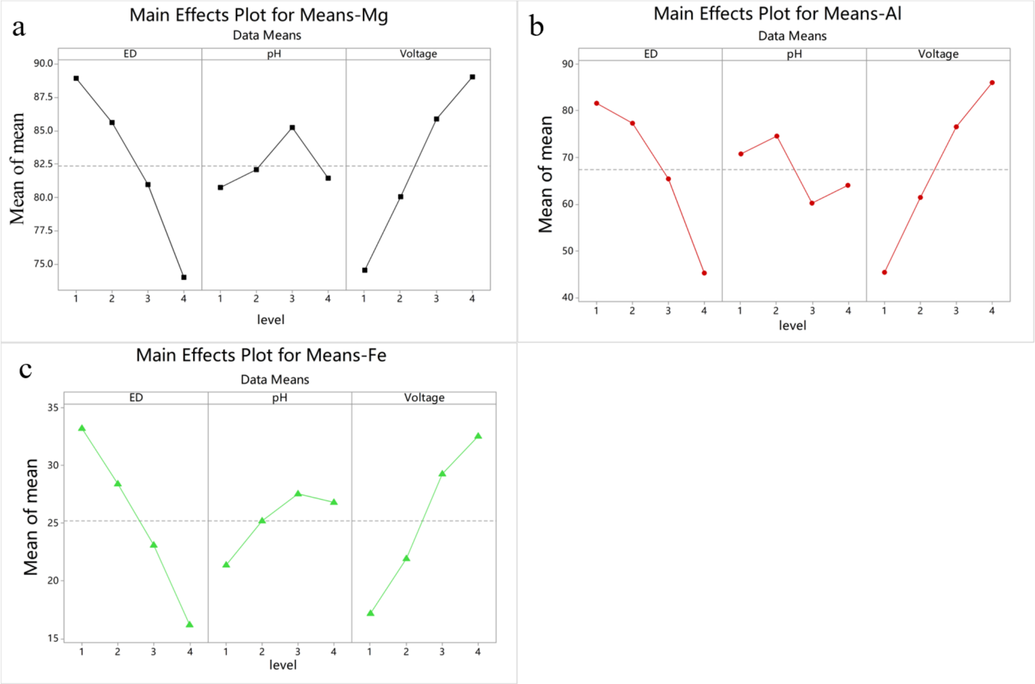

Figure 4. Main effects plot for means ((**a**) Mg, (**b**) Al, and (**c**) Fe).

3.2. Single-Factor Method Analysis

Through Taguchi analysis, we could know the optimal operating level of each anode, but we did not follow consideration of the energy consumption. The EC process requires energy consumption, and energy consumption was directly related to the cost of treatment and the possibility of actual operation [50,51]. So next, single-factor method analysis will be performed on the results of Taguchi test analysis combined with energy consumption to investigate the optimal conditions for TP removal in actual operation.

3.2.1. Effects of ED

The ED was an important factor for TP removal, because it can influence the electrostatic field between the anode and cathode [52]. The effects of ED on the TP removal are shown in Figure 5.

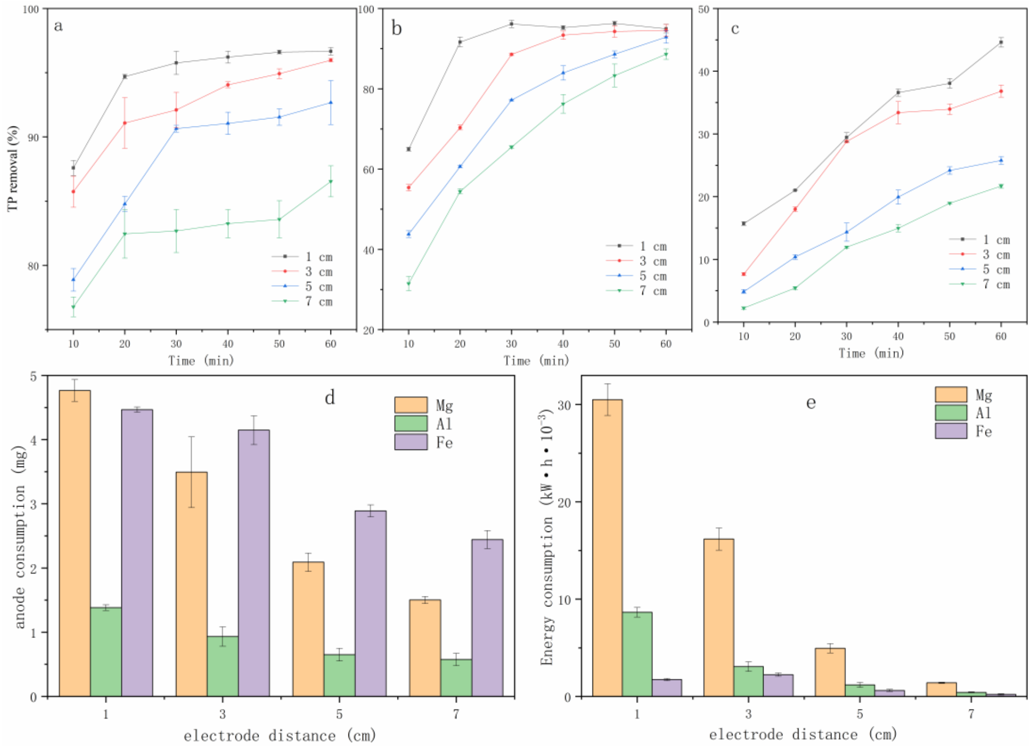

Figure 5. Effects of ED on the TP removal (**a**) Mg anode at voltage = 5 V and pH = 7, (**b**) Al anode at voltage = 5 V and pH = 5, and (**c**) Fe anode at voltage = 5 V and pH = 7, (**d**) anode consumption of three anodes, and (**e**) the energy consumption of three anodes under optimal ED.

Figure 5a compares the effects of different EDs on the removal of TP by Mg from 1 cm to 7 cm. It was obvious that the final TP removal efficiency of 1 cm ranks first at 96.67%, followed by 3 cm at 95.98%, 5 cm at 92.67%, and 7 cm at 86.54%. After 60 min, there was a slight difference in the TP removal efficiency between 1 cm and 3 cm: only 0.71%. As Figure 5b shows, there were different ED effects on TP removal by Al. Same as Mg, the larger the ED, the smaller the removal efficiency. In case of 1 cm, at the first 10 min, TP removal increases quickly at 64.95%, followed by 30 min at 96.16% and then keep stable. Compared with 1 cm, the ED was raised to 3 cm, and the final removal of TP only increases by 0.4%. The effects of 5 cm and 7 cm were near 3 cm, but require more time for treatment. As shown in Figure 5c, the trend of TP removal efficiency by Fe was the same as Mg and Al, and it was clear that overall, removal effect was not significant, and the best removal effect is only 44.61%. The mass consumption of the three anodes is shown in Figure 5d. It was clear that anode consumption decreases with increasing ED. The consumption of Mg decreased from 4.766 mg for 1 cm to 1.503 mg for 7 cm. When ED was increased from 1 cm to 7 cm, the anode consumption of Al was reduced by 0.808 mg, and Fe was 0.202 mg. In the case of ED of 3 cm, the mass consumption of Fe was 4.147 mg, Mg was 3.492 mg, and Al was 0.934 mg.

Considering energy consumption, the optimum ED would be 3 cm of three anodes, as shown in Figure 5e. In case of 3 cm, TP removal of Mg ranks first at 95.98%, followed by Al at 94.57%, and Fe at 36.83%. The removal efficiency of Mg and Al was only different by 1.41%, but the consuming of energy was about three times. Compared with Mg and Al, Fe anode consumed less energy, but the handle efficiency was low.

It can be summarized that the optimum ED of the three anodes was 3 cm. Compared with an ED of 1 cm, 3 cm not only saves energy, but also consumes less anode. Compared with EDs of 5 cm and 7 cm, the ED of 3 cm was small. The small electrostatic effect result ions move slowly [53]. This provides additional time for the metal hydrate to form flocs, resulting in an increase in the efficiency of TP removal [54], and some researchers found that smaller EDs usually contribute to improving the performance of EC [50,55,56]. When further increasing the ED from 3 cm to 7 cm, the move time of metal ions was increased and electrostatic attraction was decreased, therefore resulting in the lesser efficiency of TP removal [57]. In addition, a larger plate spacing inevitably increases the resistivity between the electrodes and narrows the efficiency of the electrodes, which also hinders the generation of metal ions [58].

3.2.2. Effects of Voltage

Voltage was a significant parameter for TP removal during the EC process [59]. Higher voltage results in higher current through solution, and the higher current could generate more metal ions into solution [60]. The effects of voltage on the TP removal are presented in Figure 6.

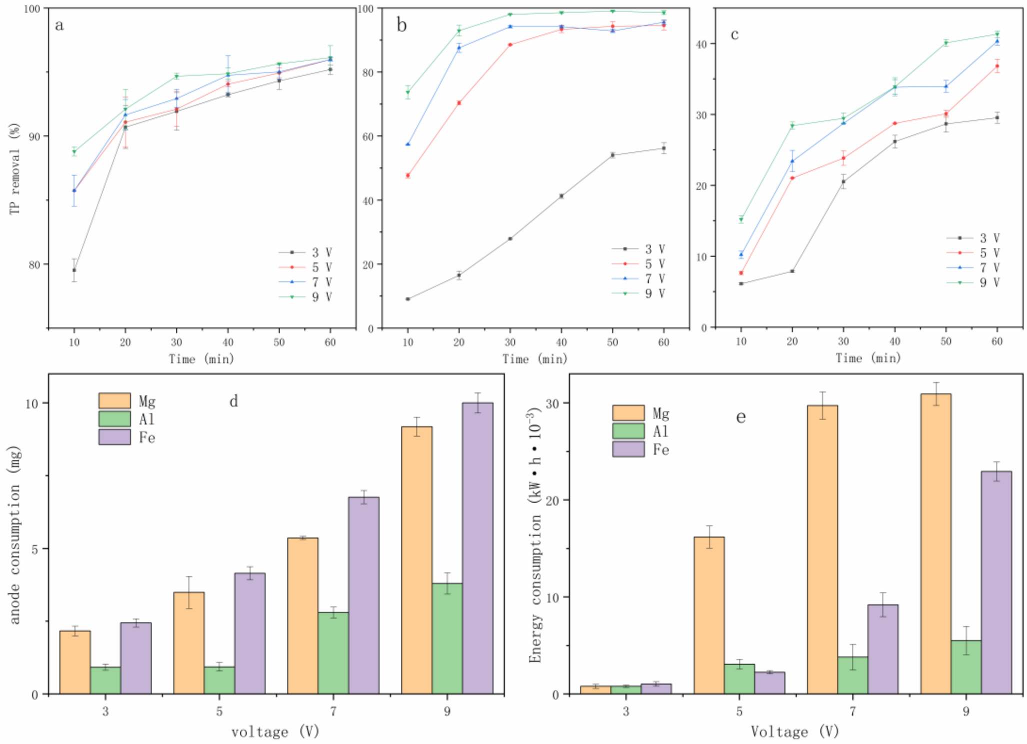

Figure 6. Effects of voltage on the TP removal (**a**) Mg anode at ED = 3 cm and pH = 7, (**b**) Al anode at ED = 3 cm and pH = 5, (**c**) Fe anode at ED = 3 cm and pH = 7, (**d**) the anode consumption of three anodes, and (**e**) the energy consumption of three anodes under optimal voltage.

As Figure 6a shows, an increase in the voltage accelerated the efficiency of TP removal by Mg. Beginning at 10 min, the slowest removal took place in a voltage of 3 V, where the TP removal reached 79.51%. Meanwhile, the voltage of 9 V ranks first at 89.15%, followed by 7 V at 85.74% and 5 V at 85.72%. As Figure 6b shows, it is clear that the optimal voltage of Al for TP removal was 9 V. The quickest removal efficiency reached 98.02% in less than 30 min. At the same time, the efficiency of 3 V is at 27.89%, 5 V is at 88.55%, and 7 V is at 94.12%. As Figure 6c shows, it is obvious that the treatment efficiency of Fe was not significant, the bigger removal efficiency was 41.32%, and the trend of TP removal was as same as Mg and Al. As Figure 6d shows, it was clear that anode consumption increases with increasing voltage. When the voltage was increased from 3 V to 9 V, the anode of Fe increased 7.558 mg, Mg was 7.021 mg, and Mg was 2.879 mg. In the case of 5 V, the consumption of Fe was 4.147 mg, which was 4.4 times the consumption of Al and 1.2 times the consumption of Mg. As Figure 6e shows, it compares the energy consumption of three metal anodes at different voltages. In the case of 5 V of voltage, the efficiency of Mg was approximately five times that of Al and eight times that of Fe. Compared with Mg, for Al, not only the treatment effect was similar at a voltage of 5 V, but it also has energy and anode consumption advantages. As for Fe, the effect of TP removal was negligible. Therefore, Al was the optimal choice for TP removal in the voltage ranging from 3 V to 9 V.

Through first-order and second-order kinetics model analyses (Table S7), it could be possible to conclude that the TP removal of Mg and Fe was best for conforming to second-order with good $R^2 > 0.98$, and Al conforming to first-order. These values indicate that the removal of TP from wastewater by Mg and Al mainly depends on chemical adsorption, and the removal of TP from wastewater by Fe mainly depends on physical adsorption [48].

3.2.3. Effects of Initial pH

The initial pH was an important factor for TP removal, because it will influence the dissolution of anode and the existence of hydrate hydroxides in the solution [61,62]. The effects of the initial pH on the TP removal are shown in the Figure 7.

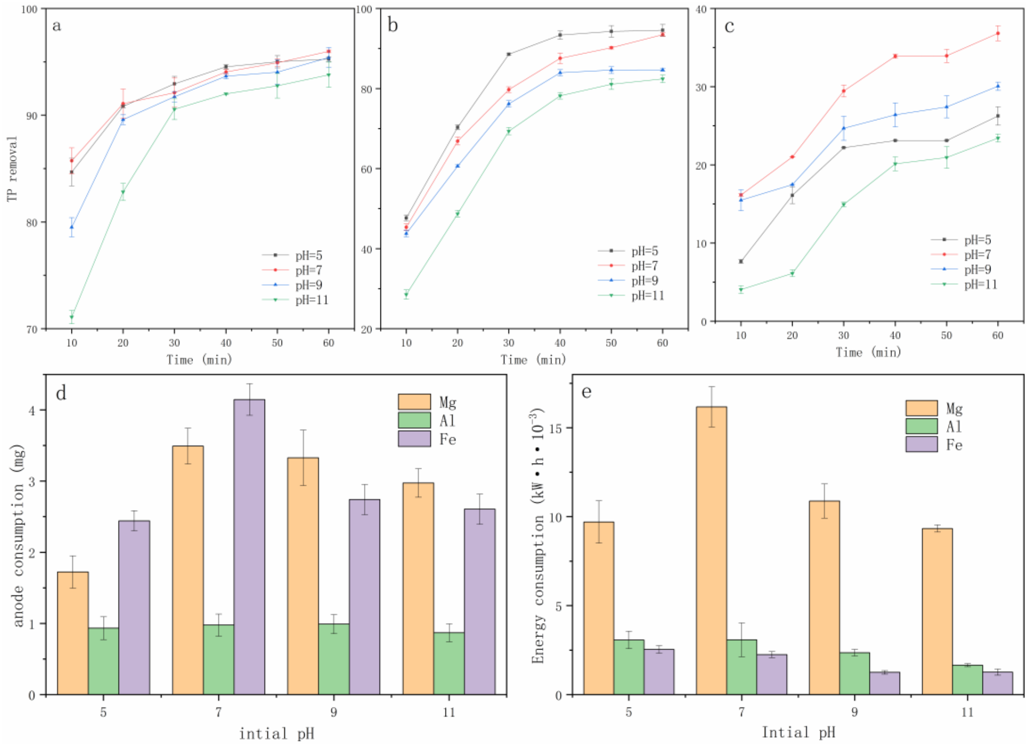

Figure 7. Effects of initial pH on the TP removal (**a**) Mg anode at ED = 3 cm and voltage = 5 V, (**b**) Al anode at ED = 3 cm and voltage = 5 V, (**c**) Fe anode at ED = 3 cm and voltage = 5 V, (**d**) the anode consumption of three anodes, and (**e**) the energy consumption of three anodes under optimal initial pH.

As shown in Figure 7a, as for Mg, the final efficiency of TP removal was more than 93%. When the initial pH increases from 5 to 7, the efficiency of TP removal increases, and achieves the maximum value 95.98%.

This could because at the initial pH of 5, there was a lot of H^+ in the solution. For Mg^{2+}, it was difficult to form hydrate hydroxides for TP removal. When the pH value increases from 7 to 9 and 11, the efficiency of TP removal decreases. This could be because at an initial pH of 7, Mg^{2+} could form precipitation with phosphate; but when pH > 7, there is numerous OH^-, and it will combine with Mg^{2+} to form precipitation and reduce the content of Mg^{2+} in the solution, thereby reducing the removal rate of TP. As shown in Figure 7b, in the case of the Al anode, the final efficiency of TP removal was more than 82.42%. As the initial pH increases, the removal efficiency decreases. The maximum removal efficiency was 94.57% at the initial pH of 5, and aluminum ions are available in a hydrolyzed state, including Al^{3+}, $Al(OH)^{2+}$, and $Al(OH)_2^+$ [63]. The specific surface area of the flocs formed by this form of aluminum ions was small, and the ability to bind to phosphate was weak, resulting in inadequate removal of phosphate. Thus, in acidic conditions, the aluminum ions destabilize the colloidal particles via neutralizing the superficial charges of phosphate. In neutral or weakly alkaline conditions, Al^{3+} could form hydrate hydroxides adsorption phosphate, but TP removal was in decline. Thus the optimal pH for Al removal TP was 5, and Kuo et al. [64] had the same result. Figure 7c compares the effects of different initial pH on the removal of TP by Fe from 5 to 11. At a pH of 5, TP removal was finally 26.26%. This efficiency of TP removal increased to the maximum 36.83% at a pH of 7. The rate of TP removal decreased steeply to 30.06% at a pH of 9, and continued to reduce gradually by 23.43%.

In the case of Fe, the complexes had a tendency to polymerize at pH 3.5–7.0. Insoluble metal hydroxides formed as there was an increase in the solution pH, which was precipitated as $Fe(OH)_2$ and $Fe(OH)_3$, respectively [37]. In addition, $Fe(OH)_3$ has poor solubility in the pH range of 4 to 7, which was good for removing phosphate from water. When the pH is 4~7, $Fe(OH)_3$ can promote the formation of positively charged hydroxides and can effectively adsorb $H_2PO_4^{-}$ and HPO_4^{2-}. Pulkka, S et al. [65] also reached the same conclusion. When the pH was greater than 10, the $Fe(OH)_4^{-}$ formed during the EC was soluble, which was not conducive to the adsorption of phosphate [66]. Thus, the optimum operating pH for CFW was 7. Jimenez et al. [67] also had the same result.

In addition, the consumption of anodes at different pH levels was also investigated. As Figure 7d shows, it was obvious that the anode consumption of the three metal anodes was the largest when the pH was 7, 5, and 7, respectively, and at acidic or neutrality conditions, the solubility of phosphate was higher, and the coagulant made it easier to capture phosphorus [68]. At the same time, according to the study of Song et al. [69], it was demonstrated that low pH was beneficial to the removal of phosphate. It was clear that the TP removal efficiency of Mg was the best. This is because Mg has a reduced negative potential [70], and it was hard to form a protective film on its surface. In the case of power, it can quickly dissolve Mg^{2+} into the solution, but the energy consumption of Mg was the maximum. The energy consumption of Mg was almost over five times as many consumed as Al, as Figure 7e shows. Under optimal reaction conditions, there was a slight difference in the final removal rate of TP between Mg and Al of only 1.41%. As for Fe, it has one thing in common with Mg in the optimal initial pH value. However the optimal TP removal of Fe was about a quarter as many as Mg.

TP mainly includes phosphate (PO_4^{3-}), hydrogen phosphate (HPO_4^{2-}), and dehydration phosphate (H_2PO^{4-}) [71]. Phosphate is available in the form of $H_2PO_4^{-}$, HPO_4^{2-}, and PO_4^{3-} at pH of 5~7, 7~10 and >12.5, respectively [72]. When pH was 10~12, HPO_4^{2-} was dominant over PO_4^{3-} in the solution.

3.3. Actual Cattle Farm Wastewater Removal Effect

Through single-factor method analysis, the optimal operating conditions could be summarized. In order to verify the application of the optimal conditions in practice, an ACFW experiment was studied, and the result is shown in Figure 8.

Figure 8a was the product of TP concentration under the optimal conditions of the Taguchi method result (T). As the picture shows, the final TP removal efficiency of Mg and Al was close, followed by Fe. The TP concentration of the single-factor method result (S) is given in Figure 8b, the ranking of the removal effects of the three metal anodes on TP was the same as the result obtained by the Taguchi method. In comparing the best conditions of the two methods in the application of ACFW, it could be summarized that the final removal of three anodes was near. However, T has a better COD removal effect than S, as Figure 8c shows. This may be because T consumed more energy, as Figure 8d shows. Consider the cost in actual use in the straightforward calculation of the cost of power consumption in two methods in actual operation. The electrical energy price in Shihezi was 0.0643 USD·kW·h. The case of Mg under T was 2.8 times as many as S, Al was 1.9 times, and Fe was 1.2 times. Under the best conditions of single factor for three anodes, the TP removal effect per unit of the Mg was 1.56 times the Fe and 2.59 times the Al. Therefore, the most cost-effective way to remove TP in ACFW was the Al under S.

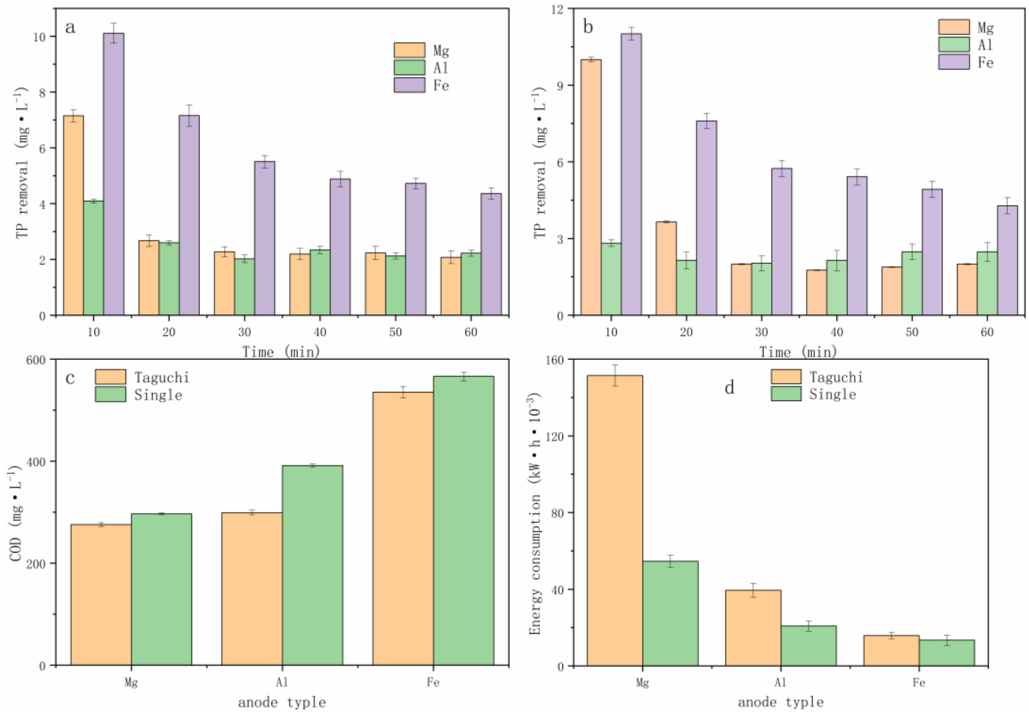

Figure 8. CFW treatment effect diagram ((**a**) the content of TP under the optimal conditions of the Taguchi method, (**b**) the content of TP under the optimal condition of the single method, (**c**) the COD content in CFW, (**d**) the energy consumption of CFW.

Meanwhile, the SEM images and EDX elemental spectra of precipitate were set out in Figure 9.

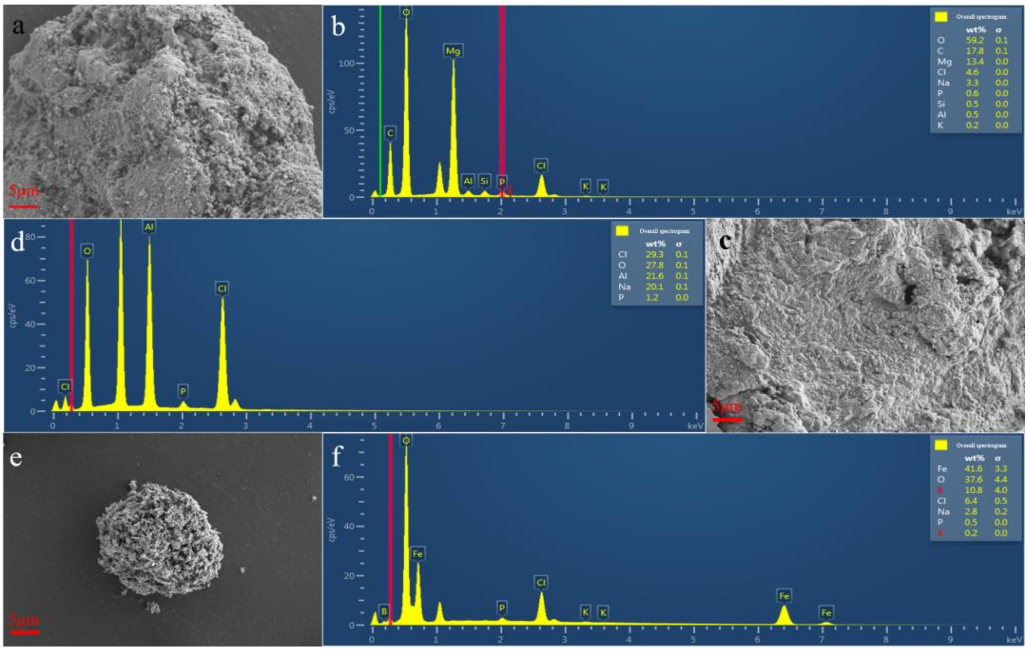

Figure 9. SEM and EDX images of the product under optimal single-factor conditions ((**a**) the SEM of Mg, (**b**) the EDX of Mg, (**c**) the SEM of Al, (**d**) the EDX of Al, (**e**), the SEM of Fe, and (**f**) the EDX of Fe).

The SEM images of the precipitate revealed that the precipitate surface of Mg and Al formed a large number of grooves (Figure 9a,c), which may be the active sites for TP removal: three EDX spectra, the appearance of phosphorous peak instruction, and the successful removal of TP. Figure 9b shows the peak with contents of oxygen (O), carbon (C), magnesium, chlorine (Cl), sodium (Na), phosphorus (P), silicon (Si), aluminum, and potassium (K), where the presence of elements such as Si, aluminum, and K was obvious. This may be in addition to reducing impurities in industrial magnesium electrodes and improving the conductivity of magnesium electrodes used in the manufacturing process. The presence of the elements magnesium, K, O, Cl, and Na was understandable because of the Mg electrode, phosphorus (KH_2PO_4), and electrolyte (NaCl). The C element may be from the organic matter in ACFW. The elemental composition of Al deposits investigated using EDX demonstrates the presence of Cl, O, aluminum, and Na as primary elements, as Figure 9d shows. O and boron (B) elements were the main elements in the ACFW sediments treated by Fe, as shown in Figure 9f. The appearance of B was caused by impurities in the iron electrode. In summary, the conditions obtained by using S entered into force for the ACFW treatment.

4. Conclusions

In this study, the removal of TP of CFW was investigated using an electrocoagulation process in which we used three different metal anodes and analyzed them through the Taguchi method and single-factor method. Compared to the other two anodes, the Al is not only energy friendly, but also has an excellent processing effect; so aluminum electrode is the best electrode. Among the three parameters, ED has the greatest impact on the response, followed by voltage and initial pH. Voltage could significantly influence the efficiency of magnesium anode and aluminum anode in removing TP. Through single-factor analysis, it could be summarized that the optimal operating conditions of Mg and Fe were electrode distance = 3 cm, pH = 7, and voltage = 5 V, Al was electrode distance = 3 cm, pH = 5, and voltage = 5 V. It was verified by ACFW that this condition could well remove the TP, and the flocs produced by the three electrodes mainly remove the TP in the wastewater by adsorption.

In the research, the removal conditions in actual wastewater were only evaluated from the perspective of energy consumption, anode consumption, and COD removal. However, there are many other indicators that must be considered in actual engineering applications. In this case, further studies are needed to combine an additional evaluation index.

Supplementary Materials: The following supporting information can be downloaded at: https://www.mdpi.com/article/10.3390/w15234134/s1, Table S1. The average Range analysis of TP removal by Mg; Table S2. The average Range analysis of TP removal by Al; Table S3. The average Range analysis of TP removal by Fe; Table S4. The average Range analysis of anode consumption by Mg; Table S5. The average Range analysis of anode consumption by Al; Table S6. The average Range analysis of anode consumption by Fe; Table S7. Kinetic analysis of the effect of electrode spacing on TP removal.

Author Contributions: Conceptualization, J.L. and P.C.; methodology, N.X.; writing—review and editing, P.C. All authors have read and agreed to the published version of the manuscript.

Funding: Financial support from the National Natural Science Foundation of China (52260002), the Special application science and technology project of the Xinjiang Bingtuan (QS2022008, 2022C19, 2021C14, 2021AB024), the High-Level Talent Research Launch Project of Shihezi University (RCZK202316) are gratefully acknowledged.

Data Availability Statement: Data are unavailable due to privacy.

Acknowledgments: We acknowledge the Jiankang Wang, Wenying Qu and Wenhuai Wang for providing the experimental facilities and discussing the draft.

Conflicts of Interest: The authors declare no conflict of interest.

References

1. Wen, S.L.; Wang, H.W.; Wu, T.; Yang, J.; Jiang, X.; Zhong, J.C. Vertical profiles of phosphorus fractions in the sediment in a chain of reservoirs in North China: Implications for pollution source, bioavailability, and eutrophication. *Sci. Total Environ.* **2019**, *704*, 10. [CrossRef] [PubMed]
2. Pruss, A.; Kay, D.; Fewtrell, L.; Bartram, J. Estimating the burden of disease from water, sanitation, and hygiene at a global level. *Environ. Health Perspect.* **2002**, *110*, 537–542. [CrossRef] [PubMed]
3. Lang, Z.C.; Zhou, M.H.; Zhang, Q.Z.; Yin, X.Y.; Li, Y.W. Comprehensive treatment of marine aquaculture wastewater by a cost-effective flow-through electro-oxidation process. *Sci. Total Environ.* **2020**, *722*, 9. [CrossRef]
4. Wei, J.; Meng, X.; Wen, X.; Song, Y. The Second National Pollution Source Census Bulletin. Available online: https://www.mee.gov.cn/xxgk2018/xxgk/xxgk01/202006/W020200610353985963290 (accessed on 8 June 2020).
5. Wu, Y.; Li, X.; Yang, Q.; Wang, D.; Xu, Q.; Yao, F.; Chen, F.; Tao, Z.; Huang, X. Hydrated lanthanum oxide-modified diatomite as highly efficient adsorbent for low-concentration phosphate removal from secondary effluents. *J. Environ. Manag.* **2018**, *231*, 370–379. [CrossRef] [PubMed]
6. Wei, J.; Meng, X.; Wen, X.; Song, Y. Adsorption and recovery of phosphate from water by amine fiber, effects of co-existing ions and column filtration. *J. Environ. Sci.* **2019**, *87*, 123–132. [CrossRef] [PubMed]
7. Cao, J.; Yang, Z.-H.; Xiong, W.-P.; Zhou, Y.-Y.; Peng, Y.-R.; Li, X.; Zhou, C.-Y.; Xu, R.; Zhang, Y.-R. One-step synthesis of Co-doped UiO-66 nanoparticle with enhanced removal efficiency of tetracycline: Simultaneous adsorption and photocatalysis. *Chem. Eng. J.* **2018**, *353*, 126–137. [CrossRef]
8. Barca, C.; Gerente, C.; Meyer, D.; Cliazarenc, F.; Andres, Y. Phosphate removal from synthetic and real wastewater using steel slags produced in Europe. *Water Res.* **2012**, *46*, 2376–2384. [CrossRef]
9. Akram, M.; Xu, X.; Gao, B.Y.; Yue, Q.Y.; Shang, Y.N.; Khan, R.; Inam, M.A. Adsorptive removal of phosphate by the bimetallic hydroxide nanocomposites embedded in pomegranate peel. *J. Environ. Sci.* **2020**, *91*, 189–198. [CrossRef]
10. Xiong, W.; Tong, J.; Yang, Z.; Zeng, G.; Zhou, Y.; Wang, D.; Song, P.; Xu, R.; Zhang, C.; Cheng, M. Adsorption of phosphate from aqueous solution using iron-zirconium modified activated carbon nanofiber: Performance and mechanism. *J. Colloid Interface Sci.* **2017**, *493*, 17–23. [CrossRef]
11. Wu, B.; Fang, L.; Fortner, J.D.; Guan, X.; Lo, I.M.C. Highly efficient and selective phosphate removal from wastewater by magnetically recoverable La(OH)(3)/Fe_3O_4 nanocomposites. *Water Res.* **2017**, *126*, 179–188. [CrossRef]
12. Koilraj, P.; Sasaki, K. Selective removal of phosphate using La-porous carbon composites from aqueous solutions: Batch and column studies. *Chem. Eng. J.* **2017**, *317*, 1059–1068. [CrossRef]
13. Huang, H.; Liu, J.; Ding, L. Recovery of phosphate and ammonia nitrogen from the anaerobic digestion supernatant of activated sludge by chemical precipitation. *J. Clean. Prod.* **2015**, *102*, 437–446. [CrossRef]
14. Kubar, A.A.; Huang, Q.; Sajjad, M.; Yang, C.; Lian, F.; Wang, J.; Kubar, K.A. The Recovery of Phosphate and Ammonium from Biogas Slurry as Value-Added Fertilizer by Biochar and Struvite Co-Precipitation. *Sustainability* **2021**, *13*, 3827. [CrossRef]
15. Jabari, P.; Munz, G.; Oleszkiewicz, J.A. Selection of denitrifying phosphorous accumulating organisms in IFAS systems: Comparison of nitrite with nitrate as an electron acceptor. *Chemosphere* **2014**, *109*, 20–27. [CrossRef] [PubMed]
16. Yuan, Q.; Oleszkiewicz, J. Selection and enrichment of denitrifying phosphorus accumulating organisms in activated sludge. *Desalination Water Treat.* **2010**, *22*, 72–77. [CrossRef]
17. Gomez, S.; Felipe Hurtado, C.; Orellana, J. Bioremediation of organic sludge from a marine recirculating aquaculture system using the polychaete Abarenicola pusilla (Quatrefages, 1866). *Aquaculture* **2019**, *507*, 377–384. [CrossRef]
18. Davidson, J.; Helwig, N.; Summerfelt, S.T. Fluidized sand biofilters used to remove ammonia, biochemical oxygen demand, total coliform bacteria, and suspended solids from an intensive aquaculture effluent. *Aquac. Eng.* **2008**, *39*, 6–15. [CrossRef]
19. Moussa, D.T.; El-Naas, M.H.; Nasser, M.; Al-Marri, M.J. A comprehensive review of electrocoagulation for water treatment: Potentials and challenges. *J. Environ. Manag.* **2016**, *186*, 24–41. [CrossRef]
20. Keyikoglu, R.; Can, O.T.; Aygun, A.; Tek, A. Comparison of the effects of various supporting electrolytes on the treatment of a dye solution by electrocoagulation process. *Colloid Interface Sci. Commun.* **2019**, *33*, 100210. [CrossRef]
21. Thirugnanasambandham, K.; Sivakumar, V.; Maran, J.P. Optimization of process parameters in electrocoagulation treating chicken industry wastewater to recover hydrogen gas with pollutant reduction. *Renew. Energy* **2015**, *80*, 101–108. [CrossRef]
22. Yetilmezsoy, K.; Ilhan, F.; Sapci-Zengin, Z.; Sakar, S.; Gonullu, M.T. Decolorization and COD reduction of UASB pretreated poultry manure wastewater by electrocoagulation process: A post-treatment study. *J. Hazard. Mater.* **2008**, *162*, 120–132. [CrossRef]
23. Uen, U.T.; Koparal, A.S.; Oeguetveren, U.B. Hybrid processes for the treatment of cattle-slaughterhouse wastewater using aluminum and iron electrodes. *J. Hazard. Mater.* **2008**, *164*, 580–586. [CrossRef]
24. Costa, C.R.; Olivi, P. Effect of chloride concentration on the electrochemical treatment of a synthetic tannery wastewater. *Electrochim. Acta* **2008**, *54*, 2046–2052. [CrossRef]
25. Wang, C.T.; Chou, W.L.; Kuo, Y.M. Removal of COD from laundry wastewater by electrocoagulation/electroflotation. *J. Hazard. Mater.* **2008**, *164*, 81–86. [CrossRef] [PubMed]
26. Chen, X.; Chen, G.; Yue, P.L. Separation of pollutants from restaurant wastewater by electrocoagulation. *Sep. Purif. Technol.* **2000**, *19*, 65–76. [CrossRef]
27. Chen, Y.; Baygents, J.C.; Farrell, J. Evaluating electrocoagulation and chemical coagulation for removing dissolved silica from high efficiency reverse osmosis (HERO) concentrate. *J. Water Process Eng.* **2016**, *16*, 50–55. [CrossRef]

28. Landels, A.; Beacham, T.A.; Evans, C.T.; Carnovale, G.; Raikova, S.; Cole, I.S.; Goddard, P.; Chuck, C.; Allen, M.J. Improving electrocoagulation floatation for harvesting microalgae. *Algal Res.-Biomass Biofuels Bioprod.* **2019**, *39*, 101446. [CrossRef]
29. Kobya, M.; Can, O.T.; Bayramoglu, M. Treatment of textile wastewaters by electrocoagulation using iron and aluminum electrodes. *J. Hazard. Mater.* **2003**, *100*, 163–178. [CrossRef]
30. Bayramoglu, M.; Kobya, M.; Can, O.T.; Sozbir, M. Operating cost analysis of electrocoagulation of textile dye wastewater. *Sep. Purif. Technol.* **2004**, *37*, 117–125. [CrossRef]
31. Daneshvar, N.; Sorkhabi, H.A.; Kasiri, M.B. Decolorization of dye solution containing Acid Red 14 by electrocoagulation with a comparative investigation of different electrode connections. *J. Hazard. Mater.* **2004**, *112*, 55–62. [CrossRef]
32. Khemila, B.; Merzouk, B.; Chouder, A.; Zidelkhir, R.; Leclerc, J.-P.; Lapicque, F. Removal of a textile dye using photovoltaic electrocoagulation. *Sustain. Chem. Pharm.* **2017**, *7*, 27–35. [CrossRef]
33. Merzouk, B.; Gourich, B.; Madani, K.; Vial, C.; Sekki, A. Removal of a disperse red dye from synthetic wastewater by chemical coagulation and continuous electrocoagulation. A comparative study. *Desalination* **2011**, *272*, 246–253. [CrossRef]
34. Al Aji, B.; Yavuz, Y.; Koparal, A.S. Electrocoagulation of heavy metals containing model wastewater using monopolar iron electrodes. *Sep. Purif. Technol.* **2011**, *86*, 248–254. [CrossRef]
35. Kim, T.; Kim, T.-K.; Zoh, K.-D. Removal mechanism of heavy metal (Cu, Ni, Zn, and Cr) in the presence of cyanide during electrocoagulation using Fe and Al electrodes. *J. Water Process Eng.* **2019**, *33*, 101109. [CrossRef]
36. Kobya, M.; Ciftci, C.; Bayramoglu, M.; Sensoy, M.T. Study on the treatment of waste metal cutting fluids using electrocoagulation. *Sep. Purif. Technol.* **2007**, *60*, 285–291. [CrossRef]
37. Kobya, M.; Demirbas, E.; Dedeli, A.; Sensoy, M.T. Treatment of rinse water from zinc phosphate coating by batch and continuous electrocoagulation processes. *J. Hazard. Mater.* **2009**, *173*, 326–334. [CrossRef]
38. Fouad, Y.O.A.; Konsowa, A.H.; Farag, H.A.; Sedahmed, G.H. Performance of an electrocoagulation cell with horizontally oriented electrodes in oil separation compared to a cell with vertical electrodes. *Chem. Eng. J.* **2008**, *145*, 436–440. [CrossRef]
39. Liu, Y.; Chen, Y.; Jiang, W.; Wang, T. Experimental Study on the Treatment of Oily Wastewater by Electrocoagulation with Aluminum Electrodes at Different Heights. *J. Electrochem. Soc.* **2019**, *166*, E533–E541. [CrossRef]
40. Nasrullah, M.; Zularisam, A.W.; Krishnan, S.; Sakinah, M.; Singh, L.; Fen, Y.W. High performance electrocoagulation process in treating palm oil mill effluent using high current intensity application. *Chin. J. Chem. Eng.* **2018**, *27*, 208–217. [CrossRef]
41. Yang, C.-L. Electrochemical coagulation for oily water demulsification. *Sep. Purif. Technol.* **2006**, *54*, 388–395. [CrossRef]
42. Min, G.; Yirong, Z.; Jinglong, Z.; Liming, W.; Hongwei, Z.; Lei, S. Study on phosphorous removal by electrolytic process with iron electrode. *Technol. Water Treat.* **2014**, *40*, 39–42. [CrossRef]
43. Liu, W.; Li, J.; He, X.; Wang, Z.; Zhao, C. Factors Influencing the Removal of Phosphorus and the Purity of Recycling Struvite in Wastewater by the Electrochemical Sacrificial Magnesium Anode Method. *Sci. Adv. Mater.* **2019**, *11*, 128–134. [CrossRef]
44. Mores, R.; Treichel, H.; Zakrzevski, C.A.; Kunz, A.; Steffens, J.; Dallago, R.M. Remove of phosphorous and turbidity of swine wastewater using electrocoagulation under continuous flow. *Sep. Purif. Technol.* **2016**, *171*, 112–117. [CrossRef]
45. Kobya, M.; Gengec, E.; Sensoy, M.T.; Demirbas, E. Treatment of textile dyeing wastewater by electrocoagulation using Fe and Al electrodes: Optimisation of operating parameters using central composite design. *Color. Technol.* **2014**, *130*, 226–235. [CrossRef]
46. Kirujika, K.; Kreshaanth, S.; Gunathilake, C.; Udagedara, T.; Manipura, A. Investigation of electrochemical denitrification of prawn-farm wastewater. *Sep. Sci. Technol.* **2020**, *8*, 2862–2869. [CrossRef]
47. Jia, G.; Jing, H.; Hu, B.; Ju, Z. *Water and Wastewater Monitoring and Analysis Methods*, 4th ed.; China Environmental Science Press: Beijing, China, 2002.
48. Tohamy, H.S.; El-Sakhawy, M.; Kamel, S. Microwave-assisted synthesis of amphoteric fluorescence carbon quantum dots and their chromium adsorption from aqueous solution. *Sci. Rep.* **2023**, *13*, 11306. [CrossRef]
49. Shapiro, S.; Francia, R. An Approximate Analysis of Variance Test for Normality. *J. Am. Stat. Assoc.* **1972**, *67*, 215–216. [CrossRef]
50. Brahmi, K.; Bouguerra, W.; Hamrouni, B.; Elaloui, E.; Loungou, M.; Tlili, Z. Investigation of electrocoagulation reactor design parameters effect on the removal of cadmium from synthetic and phosphate industrial wastewater. *Arab. J. Chem.* **2014**, *12*, 1848–1859. [CrossRef]
51. Hashim, K.S.; Shaw, A.; Al Khaddar, R.; Pedrola, M.O.; Phipps, D. Iron removal, energy consumption and operating cost of electrocoagulation of drinking water using a new flow column reactor. *J. Environ. Manag.* **2016**, *189*, 98–108. [CrossRef]
52. Emamjomeh, M.M. Electrocoagulation as a green technology for phosphate removal from river water. *Sep. Purif. Technol.* **2019**, *217*, 85. [CrossRef]
53. Han, Z.Y.; Wang, L.; Duan, L.; Zhu, S.M.; Ye, Z.Y.; Yu, H.J. The electrocoagulation pretreatment of biogas digestion slurry from swine farm prior to nanofiltration concentration. *Sep. Purif. Technol.* **2016**, *156*, 817–826. [CrossRef]
54. Bazrafshan, E.; Mohammadi, L.; Ansari-Moghaddam, A.; Mahvi, A.H. Heavy metals removal from aqueous environments by electrocoagulation process—A systematic review. *J. Environ. Health Sci. Eng.* **2015**, *13*, 16. [CrossRef] [PubMed]
55. Anand, M.V.; Srivastava, V.C.; Singh, S.; Bhatnagar, R.; Mall, I.D. Electrochemical treatment of alkali decrement wastewater containing terephthalic acid using iron electrodes. *J. Taiwan Inst. Chem. Eng.* **2013**, *45*, 908–913. [CrossRef]
56. Attour, A.; Touati, M.; Thin, M.; Ben Amor, M.; Lapicque, F.; Leclerc, J.P. Influence of operating parameters on phosphate removal from water by electrocoagulation using aluminum electrodes. *Sep. Purif. Technol.* **2013**, *123*, 124–129. [CrossRef]
57. Khandegar, V.; Saroha, A.K. Electrocoagulation for the treatment of textile industry effluent—A review. *J. Environ. Manag.* **2013**, *128*, 949–963. [CrossRef]

58. Qian, F.; Zhang, K.J.; Liu, X.H.; Guan, W.Y.; Chen, X.D.; Song, L.R.; Fang, F.; Luo, J.Y.; Xue, Z.X.; Cao, J.S. An improved kinetic model for dephosphorization of laundry wastewater by electrocoagulation. *J. Water Process Eng.* **2020**, *39*, 8. [CrossRef]
59. Huang, H.M.; Zhang, D.D.; Guo, G.J.; Jiang, Y.; Wang, M.S.; Zhang, P.; Li, J. Dolomite application for the removal of nutrients from synthetic swine wastewater by a novel combined electrochemical process. *Chem. Eng. J.* **2017**, *335*, 665–675. [CrossRef]
60. Aoudj, S.; Khelifa, A.; Drouiche, N.; Hecini, M.; Hamitouche, H. Electrocoagulation process applied to wastewater containing dyes from textile industry. *Chem. Eng. Process.-Process Intensif.* **2010**, *49*, 1176–1182. [CrossRef]
61. Bassyouni, D.G.; Hamad, H.A.; El-Ashtoukhy, E.S.Z.; Amin, N.K.; Abd El-Latif, M.M. Comparative performance of anodic oxidation and electrocoagulation as clean processes for electrocatalytic degradation of diazo dye Acid Brown 14 in aqueous medium. *J. Hazard. Mater.* **2017**, *335*, 178–187. [CrossRef]
62. Khorram, A.G.; Fallah, N. Treatment of textile dyeing factory wastewater by electrocoagulation with low sludge settling time: Optimization of operating parameters by RSM. *J. Environ. Chem. Eng.* **2017**, *6*, 635–642. [CrossRef]
63. Congcong, C.; Guanglei, Q.; Chenxin, X. Influencing factors and kinetics analysis of electrocoagulation with bipolar aluminum electrodes treating high fluorine groundwater. *Chin. J. Environ. Eng.* **2020**, *14*, 1216–1223. [CrossRef]
64. Kuokkanen, V.; Kuokkanen, T.; Ramo, J.; Lassi, U.; Roininen, J. Removal of phosphate from wastewaters for further utilization using electrocoagulation with hybrid electrodes—Techno-economic studies. *J. Water Process Eng.* **2014**, *8*, E50–E57. [CrossRef]
65. Pulkka, S.; Martikainen, M.; Bhatnagar, A.; Sillanpaa, M. Electrochemical methods for the removal of anionic contaminants from water—A review. *Sep. Purif. Technol.* **2014**, *132*, 252–271. [CrossRef]
66. Omwene, P.I.; Kobya, M. Treatment of domestic wastewater phosphate by electrocoagulation using Fe and Al electrodes: A comparative study. *Process Saf. Environ. Prot.* **2018**, *116*, 34–51. [CrossRef]
67. Jimenez, C.; Saez, C.; Martinez, F.; Canizares, P.; Rodrigo, M.A. Electrochemical dosing of iron and aluminum in continuous processes: A key step to explain electro-coagulation processes. *Sep. Purif. Technol.* **2012**, *98*, 102–108. [CrossRef]
68. Zhang, X.; Lin, H.J.; Hu, B. The effects of electrocoagulation on phosphorus removal and particle settling capability in swine manure. *Sep. Purif. Technol.* **2018**, *200*, 112–119. [CrossRef]
69. Song, X.Y.; Pan, Y.Q.; Wu, Q.Y.; Cheng, Z.H.; Ma, W. Phosphate removal from aqueous solutions by adsorption using ferric sludge. *Desalination* **2011**, *280*, 384–390. [CrossRef]
70. Donneys-Victoria, D.; Bermudez-Rubio, D.; Torralba-Ramirez, B.; Marriaga-Cabrales, N.; Machuca-Martinez, F. Removal of indigo carmine dye by electrocoagulation using magnesium anodes with polarity change. *Environ. Sci. Pollut. Res.* **2019**, *26*, 7164–7176. [CrossRef]
71. Fulazzaky, M.A.; Salim, N.A.A.; Abdullah, N.H.; Yusoff, A.R.M.; Paul, E. Precipitation of iron-hydroxy-phosphate of added ferric iron from domestic wastewater by an alternating aerobic-anoxic process. *Chem. Eng. J.* **2014**, *253*, 291–297. [CrossRef]
72. Karageorgiou, K.; Paschalis, M.; Anastassakis, G.N. Removal of phosphate species from solution by adsorption onto calcite used as natural adsorbent. *J. Hazard. Mater.* **2006**, *139*, 447–452. [CrossRef]

Disclaimer/Publisher's Note: The statements, opinions and data contained in all publications are solely those of the individual author(s) and contributor(s) and not of MDPI and/or the editor(s). MDPI and/or the editor(s) disclaim responsibility for any injury to people or property resulting from any ideas, methods, instructions or products referred to in the content.